# Surface Plasmon Coplanar Waveguides: Mode Characteristics and Mode Conversion Losses

Kyung-Young Jung, *Member, IEEE*, Fernando L. Teixeira, *Senior Member, IEEE*, and Ronald M. Reano, *Senior Member, IEEE*

***Abstract*—We investigate characteristics of modes supported by a surface plasmon (SP) coplanar waveguide (CPW) and contrast them against those of SP gap waveguide (GW) mode. We illustrate that the SP CPW can yield higher mode confinement versus the SP GW. In addition, we analyze 90° bend structures to investigate mode conversion losses associated with discontinuities and we further propose a modified SP CPW to alleviate these losses.**

***Index Terms*—Integrated optics, optical waveguides, surface plasmons (SPs).**

## I. Introduction

SURFACE plasmon (SP) waveguides are of great interest for compact photonic integrated circuits because they can provide subwavelength confinement of guided modes. A variety of SP waveguides has been reported, including metallic nanoparticle arrays [1], [2], V-shaped grooves in metals [3], 2-D SP gap waveguides (GWs) [4], [5], and more realistic 3-D SP GWs [6]–[9]. In particular, 3-D SP GWs can yield wideband subwavelength confinement and moderate propagation length $L_p$ (the length for $1/e$ field decay) [7]. Recently, SP quasi-coplanar waveguides (QCPWs) were proposed (in which the central metal strip is vertically misaligned to other two outer metal sections) to simplify fabrication steps and the effects of geometrical parameters on mode confinement were investigated [10].

In this letter, we study an SP coplanar waveguide (CPW) without vertical misalignment. Here we focus particularly on characteristics of SP guided modes supported by the SP CPW. The results indicate that the (fundamental) even mode of the SP CPW can yield higher mode confinement compared to SP GW mode, for the same gap width and metal thickness. We further investigate mode conversion losses in the SP CPW and propose a modified SP CPW to alleviate these losses.

Manuscript received November 24, 2008; revised January 15, 2009. First published February 24, 2009; current version published April 29, 2009. This work was supported by the Air Force Office of Scientific Research (AFOSR) under MURI Grant FA 9550-04-1-0359, by the National Science Foundation (NSF) under Grant ECCS-0347502, and by OSC under Grant PAS-0061 and Grant PAS-0110.

K.-Y. Jung was with the ElectroScience Laboratory and Department of Electrical and Computer Engineering, The Ohio State University, Columbus, OH 43212 USA. He is now with the Division of Electrical and Computer Engineering, College of Information Technology, Ajou University, Suwon 443-749, Korea (e-mail: kyjung@ajou.ac.kr).

F. L. Teixeira and R. M. Reano are with the ElectroScience Laboratory and Department of Electrical and Computer Engineering, The Ohio State University, Columbus, OH 43212 USA (e-mail: teixeira@ece.osu.edu; reano@ece.osu.edu).

Color versions of one or more of the figures in this letter are available online at http://ieeexplore.ieee.org.

Digital Object Identifier 10.1109/LPT.2009.2015578

## II. Numerical Results

The analysis is performed using a finite-difference time-domain (FDTD) algorithm [11] extended to handle the Drude dispersion model (with loss) for metals, e.g., Ag in this study. The relative permittivity of Ag is described by $\epsilon_r(\omega) = \epsilon_\infty + \omega_D^2/[j\omega(\Gamma_D + j\omega)]$, with $\epsilon_\infty = 3.7$, $\omega_D = 13.8331 \times 10^{15}$ rad/s, and $\Gamma_D = 2.7362 \times 10^{13}$ rad/s [12], which is consistent with experimental data by Johnson and Christy [13]. The time-marching FDTD update equations are obtained by employing the auxiliary differential approach and introducing an equivalent Drude current term [14].

### A. SP CPW

We first illustrate the characteristics of modes supported by the SP CPW. The power density of the SP CPW with $h = w = d = 50$ nm at $\lambda_0 = 1550$ nm is shown in Fig. 1(a) and (b), where contour plots of $-10$ and $-20$ dB are also included. The SP CPW even mode (with respect to electric potential) is very well confined around the central metal strip, with stronger power density near the edges of the central metal strip. The SP CPW odd mode is not as well confined but it is still somewhat confined inside two gaps. We also plot the power density of the SP GW with $h = w = 50$ nm at $\lambda_0 = 1550$ nm in Fig. 1(c). The SP GW mode is less confined versus SP CPW even mode but more confined versus SP CPW odd mode. We illustrate mode confinement quantitatively by calculating the mode effective area $A_M$ for a $-20$-dB threshold, as shown in Table I. Note that the SP CPW is equivalent to two coupled SP GWs, leading to (even and odd) coupled modes [8], [9].

Fig. 2 shows the effective index $n_{\text{eff}}$ of SP guided modes for the SP CPW and the SP GW calculated from the propagation constant [15], where the Ag–$SiO_2$ SP mode is also included. The SP CPW even mode has higher $n_{\text{eff}}$ than the SP GW mode, indicating that the ratio [7] of the modal power in (lossy) Ag section to that in the dielectric sections is larger for the SP CPW even mode compared to the SP GW mode. As a result, the SP CPW even mode yields stronger confinement and shorter $L_p$. We observe that a decrease in the gap width $w$ leads to an increase in $n_{\text{eff}}$ for both SP CPW even mode and SP GW mode, and SP CPW even mode has still higher $n_{\text{eff}}$ than SP GW mode. It is observed that, for similar $n_{\text{eff}}$ at $\lambda_0 \approx 1550$ nm, SP CPW even mode $(w = 50\ \text{nm})$ is less dispersive than SP GW mode $(w = 25\ \text{nm})$. Therefore, SP CPW even mode is very attractive for compact optical waveguide applications. SP CPW odd mode has lower $n_{\text{eff}}$ than SP GW mode, indicating less confinement

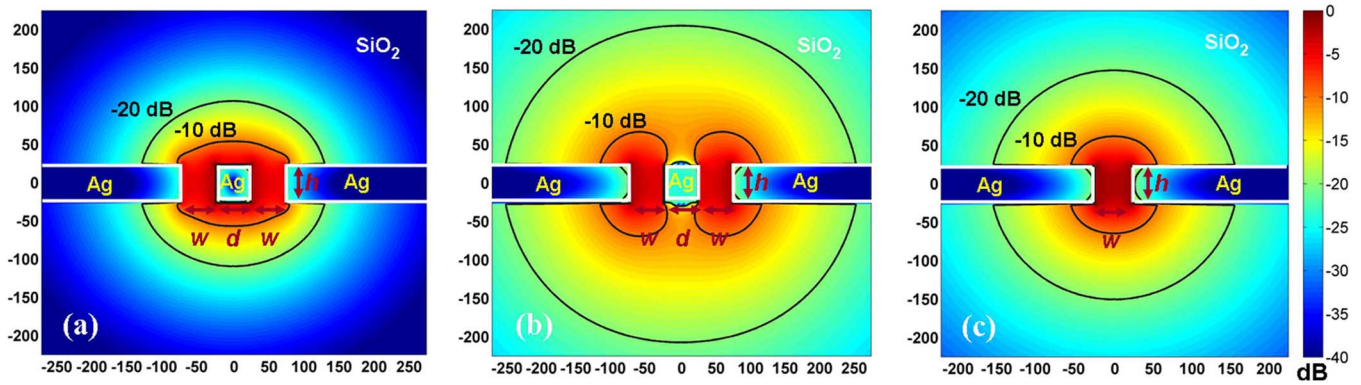


Fig. 1. Power density profile in decibel scale at $\lambda_0 = 1550$ nm for (a) SP CPW even mode, (b) SP CPW odd mode, and (c) SP GW mode. Contour plots indicating $-10$ and $-20$ dB are also included. The geometrical parameters are $h = w = d = 50$ nm for the SP CPW and $h = w = 50$ nm for the SP GW.

TABLE I
MODE CHARACTERISTICS AT $\lambda_0 = 1550$ nm

| Mode | $n_{eff}$ | $L_p$ [$\mu$m] | -20 dB $A_M$ [$10^3$nm$^2$] |
|---|---|---|---|
| SP CPW even | 2.23 | 20.14 | 40.3 |
| SP CPW odd | 1.75 | 67.5 | 147.75 |
| SP GW | 1.9 | 36.04 | 61.1 |
| SP QCPW even | 2.15 | 21.54 | 43.1 |

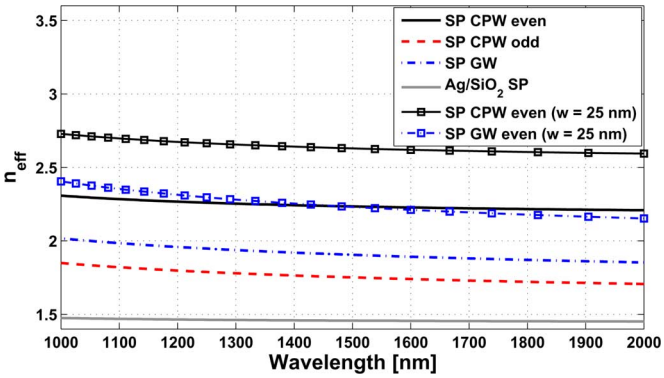


Fig. 2. Effective index $n_{\text{eff}}$ of SP guided modes for the SP CPW and the SP GW in Fig. 1. Also SP CPW even mode with $w = 25$ nm and SP GW mode with $w = 25$ nm are plotted in lines with squares.

of fields and longer $L_p$. SP CPW odd mode is suitable for longer optical waveguides. Table I summarizes mode characteristics at $\lambda_0 = 1550$ nm, including the effective index $n_{\text{eff}}$, the propagation length $L_p$, and the mode effective area $A_M$ for a $-20$-dB threshold. For comparison, the results of SP QCPW even mode (with a vertical offset of 50 nm) are also included, showing that the misalignment leads to a decrease in mode confinement, as observed in [10]. We note that when we employ a Drude dispersion model fitted to experimental data by Palik [16], we have almost a similar value of $n_{\text{eff}}$ but a decreased value of $L_p$.

Next, we investigate a 90° sharp bend structure. We consider SP CPW even mode excitation, since we are interested in compact optical waveguide applications. We measure transmittance $T$ and reflectance $R$ at 200 nm away from the discontinuity. Note that different path lengths corresponding to the two gaps at the discontinuity lead to a phase mismatch. As a consequence, SP CPW odd mode is excited and thus (even-to-odd)

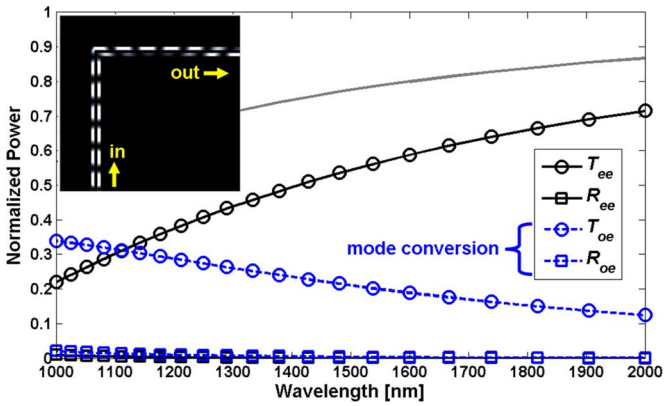


Fig. 3. Transmittance $T$ and reflectance $R$ of a 90° bend in the SP CPW. The SP GW result is also indicated in the gray line with no mark. The (top-viewing) snapshot of electric field intensity at $\lambda_0 = 1550$ nm is shown in the inset.

mode conversion losses ensue (see the inset of Fig. 3). Fig. 3 shows transmittance and reflectance, where the notation "ee" indicates "even-to-even" power ratio and "oe" indicates "even-to-odd" power ratio (i.e., mode conversion). Therefore, $T_{\text{ee}}$ and $T_{\text{oe}}$ indicate actual transmittance and mode conversion loss, respectively. As the wavelength increases, $T_{\text{ee}}$ increases but $T_{\text{oe}}$ decreases. At $\lambda_0 = 1550$ nm, $T_{\text{ee}} \approx 0.57$ and $T_{\text{oe}} \approx 0.2$. However, the SP CPW produces lower transmittance versus the SP GW due to mode conversion losses.

### *B. Modified SP CPW*

We next examine a modification of the (standard) SP CPW to reduce mode conversion losses. We ground the structure as shown in Fig. 4(a) so that the electric potentials of two outer Ag sections in the modified SP CPW coincide with each other. As a result, the modified SP CPW can greatly reduce odd mode propagation (a complete suppression is not possible because the metal does not behave as a perfect electric conductor). Fig. 4(a) shows the power density of even mode supported by the modified SP CPW with $b = 50$ nm at $\lambda_0 = 1550$ nm. The modified SP CPW has higher mode confinement ($-20$ dB $A_M = 27.19 \times 10^3$ nm$^2$) versus the standard SP CPW. Fig. 4(b) shows normalized fields along the modified SP CPW under SP CPW odd mode excitation. It is verified that the modified SP CPW can reduce odd mode propagation, especially for small $b$. In

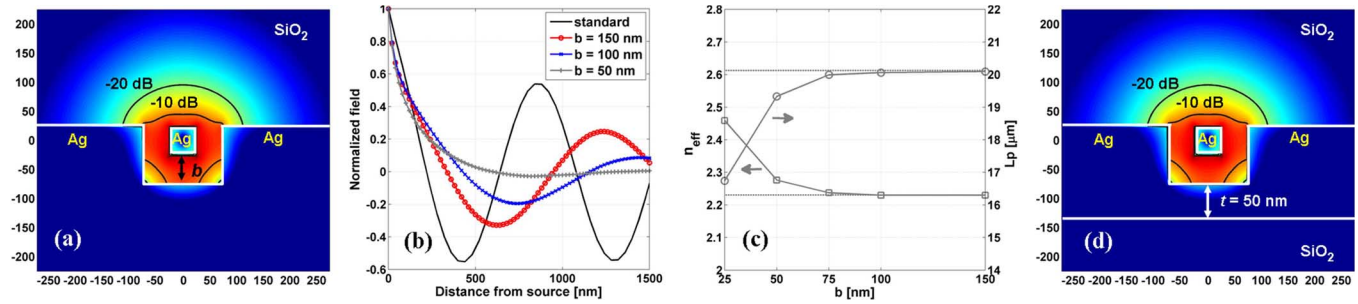


Fig. 4. SP CPW with ground connection. (a) Power density profile for SP CPW even mode in decibel scale at $\lambda_0 = 1550$ nm for $b = 50$ nm. (b) Effects of ground connection on SP CPW odd mode propagation. (c) Effects of ground connection on characteristics of SP CPW even mode (the results for the SP CPW without ground connection is indicated in horizontal black lines). (d) Same as (a) except for a vertical size reduction in ground connection structure. The depth of the ground connection can be reduced with minimal degradation in performance.

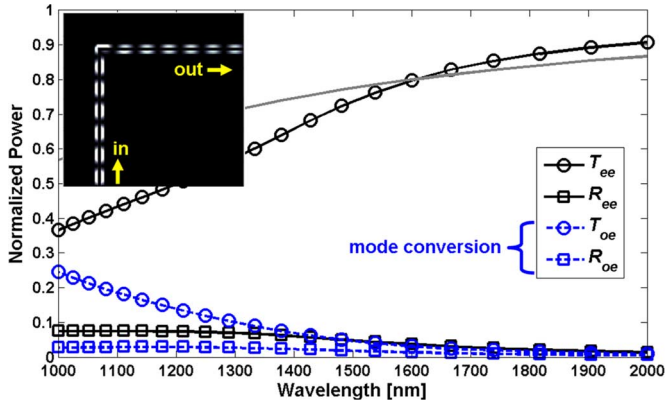


Fig. 5. Same as Fig. 3 for the SP CPW with ground connection ($b = 50$ nm).

turn, this produces less mode conversion losses at discontinuities. Fig. 4(c) shows effects of ground connection on characteristics of SP CPW even mode. Ground connection leads to an increase in $n_{\text{eff}}$ and a decrease in $L_p$ (due to the additional Ag section) and these effects are clearly observed for small $b$.

Fig. 5 shows $T_{\text{ee}}$, $T_{\text{oe}}$, and $R$ of a 90° bend in the SP CPW with ground connection ($b = 50$ nm) under even mode excitation. Compared to the standard SP CPW, the modified SP CPW produces higher $T_{\text{ee}}$ and lower $T_{\text{oe}}$, albeit with higher $R$. Electric field intensities in two metal gaps through the output port are similar to each other, indicating a near single (even) mode propagation: (compare the inset of Figs. 3 and 5). At $\lambda_0 = 1550$ nm, the SP CPW with ground connection yields $T_{\text{ee}} \approx 0.77$ and $T_{\text{oe}} \approx 0.04$. It is observed that the SP CPW produces higher transmittance compared to the SP GW for $\lambda_0 > 1600$ nm.

## III. Concluding Remarks

SP waveguides based on coplanar structures have been studied towards their use as compact (subwavelength) optical waveguides. The SP CPW supports two SP modes, viz., even mode and odd mode, and we have investigated characteristics of these modes and compared them with those of SP GW mode. SP CPW even mode can yield higher confinement of fields versus SP GW mode, being suitable for compact optical waveguide applications.

The standard SP CPW suffers from mode conversion losses at discontinuities. We modify the SP CPW by connecting two outer Ag sections and we have illustrated that ground connection reduces mode conversion losses at 90° bends and simultaneously boosts up transmittance.

## References

[1] M. Quinten, A. Leitner, J. R. Krenn, and F. R. Aussenegg, "Electromagnetic energy transport via linear chains of silver nanoparticles," *Opt. Lett.*, vol. 23, no. 17, pp. 1331–1333, Sep. 1998.

[2] K.-Y. Jung, F. L. Teixeira, and R. M. Reano, "Au/$SiO_2$ nanoring plasmon waveguides at optical communication band," *J. Lightw. Technol.*, vol. 25, no. 9, pp. 2757–2765, Sep. 2007.

[3] S. I. Bozhevolnyi, V. S. Volkov, E. Devaux, J.-Y. Laluet, and T. W. Ebbesen, "Channel plasmon subwavelength waveguide components including interferometers and ring resonators," *Nature*, vol. 440, no. 7083, pp. 508–511, Mar. 2006.

[4] R. Zia, M. D. Selker, P. B. Catrysse, and M. L. Brongersma, "Geometries and materials for subwavelength surface plasmon modes," *J. Opt. Soc. Amer. A*, vol. 21, no. 12, pp. 2442–2446, Dec. 2004.

[5] J. Shibayama, R. Takahashi, J. Yamauchi, and H. Nakano, "Frequency-dependent locally one-dimensional FDTD implementation with a combined dispersion model for the analysis of surface plasmon waveguides," *IEEE Photon. Technol. Lett.*, vol. 20, no. 10, pp. 824–826, May 15, 2008.

[6] G. Veronis and S. Fan, "Guided subwavelength plasmonic mode supported by a slot in a thin metal film," *Opt. Lett.*, vol. 30, no. 24, pp. 3359–3361, Dec. 2005.

[7] G. Veronis and S. Fan, "Modes of subwavelength plasmonic slot waveguides," *J. Lightw. Technol.*, vol. 25, no. 9, pp. 2511–2521, Sep. 2007.

[8] G. Veronis and S. Fan, "Crosstalk between three-dimensional plasmonic slot waveguides," *Opt. Express*, vol. 16, no. 3, pp. 2129–2140, Jan. 2008.

[9] D. K. Gramotnev, K. C. Vernon, and D. F. P. Pile, "Directional coupler using gap plasmon waveguides," *Appl. Phys. B*, vol. 93, no. 1, pp. 99–106, Oct. 2008.

[10] J. Kim, "Surface plasmon-polariton waveguiding characteristics of metal/dielectric quasi-coplanar structures," *Opt. Lett.*, vol. 32, no. 23, pp. 3405–3407, Dec. 2007.

[11] A. Taflove and S. C. Hagness, *Computational Electrodynamics: The Finite-Difference Time-Domain Method*, 2nd ed. Norwood, MA: Artech House, 2000.

[12] C. Sönnichsen, "Plasmons in Metal Nanostructures," Ph.D., Ludwig-Maximilians-Universtät München, München, Germany, 2001.

[13] P. B. Johnson and R. W. Christy, "Optical constants of the noble metals," *Phys. Rev. B*, vol. 6, no. 12, pp. 4370–4379, Dec. 1972.

[14] K.-Y. Jung and F. L. Teixeira, "Multispecies ADI-FDTD algorithm for nanoscale three-dimensional photonic metallic structures," *IEEE Photon. Technol. Lett.*, vol. 19, no. 8, pp. 586–588, Apr. 15, 2007.

[15] G.-C. Liang, Y.-W. Liu, and K. K. Mei, "Full-wave analysis of coplanar waveguide and slotline using the time-domain finite-difference method," *IEEE Trans. Microw. Theory Tech.*, vol. 37, no. 12, pp. 1949–1957, Dec. 1989.

[16] E. D. Palick, *Handbook of Optical Constants of Solids*. Orlando, FL: Academic, 1985.